PCCP

PAPER

View Article Online
View Journal | View Issue

CrossMark click for updates

Cite this: *Phys. Chem. Chem. Phys.*, 2015, **17**, 9519

pH-Assisted control over the binding and relocation of an acridine guest between a macrocyclic nanocarrier and natural DNA†

Mhejabeen Sayed* and Haridas Pal*

Received 17th November 2014,
Accepted 22nd February 2015

DOI: 10.1039/c4cp05335d

www.rsc.org/pccp

The differential binding affinity of the hydroxypropyl-β-cyclodextrin (HPβCD) macrocycle, a drug delivery vehicle, towards the protonated and deprotonated forms of the well-known DNA binder and model anticancer drug acridine has been exploited as a strategy for dye–drug transportation and pH-responsive delivery to a natural DNA target. From pH-sensitive changes in the ground state absorption and steady-state fluorescence characteristics of the studied acridine dye–HPβCD–DNA ternary system and strongly supported by fluorescence lifetime, fluorescence anisotropy, Job's plots, ^{1}H NMR and circular dichroism results, it is revealed that in a moderately alkaline solution (pH ∼ 8.5), the dye can be predominantly bound to the HPβCD macrocycle and when the pH is lowered to a moderately acidic region (pH ∼ 4), the dye efficiently detaches from the HPβCD cavity and almost exclusively binds to DNA. In the present study we are thus able to construct a pH-sensitive supramolecular assembly where pH acts as a simple stimulus for controlled uptake and targeted release of the dye–drug. As pH is an essential and sensitive factor in various biological processes, a simple yet reliable pH-sensitive model such as is demonstrated here can have promising applications in the host-assisted delivery of prodrug to the target sites, such as cancer or tumour microenvironments, with an enhanced stability, bioavailability and activity, and also in the design of new fluorescent probes, sensors and smart materials for applications in nano-science.

Open Access Article. Published on 26 February 2015. Downloaded on 2/25/2026 10:40:43 AM.
This article is licensed under a Creative Commons Attribution 3.0 Unported Licence.

Introduction

Supramolecular assemblies formed with the involvement of non-covalent interactions have recently attracted immense research interest due to their diverse utility in areas such as drug delivery,[1,2] nanotechnology,[3] the food industry,[4] on–off switches,[5] catalysis,[6] photostabilization,[2,7] photodynamic therapy,[8] optical sensors,[9] and many others.[10,11] The underlying non-covalent host–guest interactions have great potential for developing excellent tunable functional materials because of their strong responses to external stimuli such as pH,[1,12–15] salt,[11,15] temperature,[5,15] light,[5] *etc.* Stimuli-responsive targeted drug delivery, particularly involving macrocyclic hosts as carriers, is currently undergoing great advances in pH, salt or light acting as triggers for controlled cargo drug release at the target site for its desired effects with enhanced efficiency.[2,5,11–15] In supramolecular drug delivery applications, the drug carrier vehicle plays a vital role in transporting the drug specifically to the required location and thus increasing the concentration and also the effectiveness of the drug at the targeted site, which in turn reduces the toxicity and undesired side effects to normal cells.[1,2,13–16] Cyclodextrins (CDs) as macrocyclic hosts have been very successfully used as drug carriers in many drug formulations.[1,16,17]

CDs are unique cyclic polysaccharides formed from D-glucopyranose monomer units joined by ether linkages in a cyclic manner and thus provide hydrophobic cavities where nonpolar/hydrophobic residues of the guest molecules can be encapsulated to form inclusion complexes *via* non-covalent interactions.[7,13,18–21] Depending upon the number of D-glucopyranose units present, different CD homologues with varying cavity sizes exist, namely αCD, βCD and γCD, containing 6, 7, and 8 monomer units, respectively. Cyclodextrins and their derivatives show low toxicity, high biocompatibility and excellent inclusion capability with a variety of drug–dye molecules, which make them attractive for uses in several drug formulations and many biomedical applications.[1,2,7,8,13–17] In this regard CD derivatives with polar substituents are more promising than the parent CD hosts. For example, hydroxypropyl-β-cyclodextrin (HPβCD; Scheme 1) shows dramatically increased water solubility and much-enhanced binding interactions in comparison to parent CDs and thus can largely improve the bioavailability of the drugs. Moreover, like CDs,

Radiation & Photochemistry Division, Bhabha Atomic Research Centre, Trombay, Mumbai 400 085, India. E-mail: msayed@barc.gov.in, hpal@barc.gov.in; Fax: +91-22-25505151

† Electronic supplementary information (ESI) available: See DOI: 10.1039/c4cp05335d

Open Access Article. Published on 26 February 2015. Downloaded on 2/25/2026 10:40:43 AM.
This article is licensed under a Creative Commons Attribution 3.0 Unported Licence.

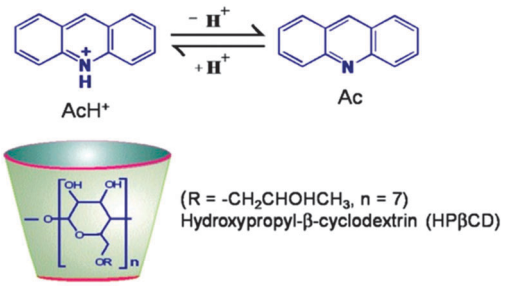

Scheme 1 The prototropic equilibrium of acridine dye and the HPβCD host used in this study are shown for quick visualization.

the HPCDs have also been reported to be well-tolerated in humans.[1,22] Recently, Huang *et al.* have reported significantly improved water solubility, thermal stability, dissolution rate and increased sprout inhibition effect in potatoes for the drug chlorpropham on complexation with HPβCD.[23] Miyake, *et al.* have also reported that the drug rutin shows increased bioavailability in a formulation made with HPβCD compared to that made with βCD.[24]

DNA is considered to be one of the primary intracellular targets for anticancer drugs, where the drug can cause selective damage of cancer cells,[25–27] taking advantage of the acidic pH conditions of the cancerous organelles.[13,28] Acridine dye and its derivatives are widely used in antitumor treatment as well as in chemotherapy. Many new acridine derivatives are being prepared, improving their DNA binding properties to give superior antitumor activity.[26,29–31] Selective delivery of such anticancer drugs at target sites that have low pH, like tumour cells, may increase the localized cytotoxicity and lower the side effects of the drug towards healthy cells.

In the present study we have investigated the interaction of the model anticancer drug acridine with HPβCD and a biomolecular target DNA at different pH conditions in aqueous solution, to find out if a pH-responsive release of the model drug to the target can be achieved. Acridine is a prototropic dye (*cf.* Scheme 1), with a pK_a of 5.4.[19] Thus, in aqueous solution it exists in the protonated form (AcH^+) at acidic pH and in neutral form (Ac) at alkaline pH.[19] Acridine and its derivatives are potent DNA binders because of their planar structures,[29,30,32] and are well-recognized as drugs showing carcinogenic effect due to their property to bind strongly with DNA. Acridine dyes are reported to exhibit two modes of binding with DNA: intercalative binding, where the planar ring of the acridines intercalates into the DNA base pairs, and semi-intercalative or exo-binding, where electrostatic interaction with the phosphate backbone of DNA plays a major role.[33–35] Significant microenvironment-sensitive changes in the spectroscopic properties of acridine dyes make them useful fluorescence probes for studying local environments in various microheterogeneous systems.[36–38] Taking advantage of the strikingly different binding behaviour of the HPβCD macrocycle towards the protonated and neutral forms of acridine dye, as observed in the present study, we have demonstrated an effective pH-triggered controlled and targeted release of the dye from the HPβCD cavity, a potential drug carrier vehicle, to the target site of DNA, which is a major goal in chemotherapeutic applications. Though the interaction of organic dyes with cyclodextrins and DNA has been reported in the literature,[39,40] detailed investigations into pH response in such supramolecular assemblies are very limited. In contrast to involved multi-step synthesis and sophisticated detection methods, we present here a simple yet reliable pH-responsive model study using photochemical measurements, which can open up new opportunities in engineering intelligent functional materials useful for various biomedical applications.

Results and discussion

1.1. Interaction of acridine dye with DNA and HPβCD hosts

1.1.1. Ground state absorption and steady-state fluorescence studies. The ground-state pK_a of acridine dye is 5.4 and both protonated (AcH^+) and neutral (Ac) forms of the dye exhibit prominent absorption and fluorescence spectral features in solution at suitable pH conditions.[19] In the steady-state (SS) fluorescence studies, both the AcH^+ and Ac forms of the dye are clearly distinguished at pH 4 and 8.5 from their characteristic fluorescence maxima at 482 nm and 430 nm, respectively. Upon addition of DNA to either of these solutions (at pH 4 and 8.5), there is a gradual decrease in the fluorescence intensity, as shown in Fig. 1a and b for

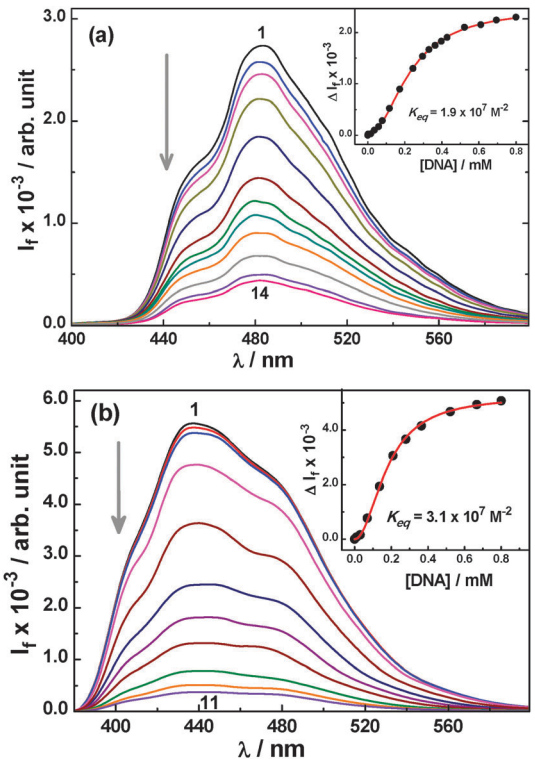

Fig. 1 (a) Changes in the SS fluorescence spectra for the AcH^+–DNA system at pH 4; [AcH^+] = 10.2 μM and [DNA] = 0, 36, 59, 78, 117, 172, 244, 296, 330, 396, 429, 522, 694 and 800 μM for spectra 1–14. Inset: fluorescence titration curve for the AcH^+–DNA system at pH 4, analysed using eqn (1) with n = 2. (b) Changes in the SS fluorescence spectra for the Ac–DNA system at pH 8.5; [Ac] = 10.5 μM and [DNA] = 0, 10, 30, 69, 135, 209, 279, 364, 522, 667 and 800 μM for spectra 1–11. Inset: fluorescence titration curve for the Ac–DNA system at pH 8.5, analysed using eqn (1) with n = 2.

This journal is © the Owner Societies 2015

Open Access Article. Published on 26 February 2015. Downloaded on 2/25/2026 10:40:43 AM.
This article is licensed under a Creative Commons Attribution 3.0 Unported Licence.

the respective cases. These results clearly indicate a strong interaction for both the prototropic forms of the dye with DNA. Changes in the fluorescence intensity (ΔI_f) with DNA concentration were correlated following eqn (1) (*cf.* Note 1, ESI†) to evaluate the binding constant (K_{eq}) for both forms of the dye:

$$\Delta I_f = \Delta I_f^{\infty} \frac{K_{eq}[B]^n}{1 + K_{eq}[B]^n} \quad (1)$$

where ΔI_f^{∞} is the final change in the fluorescence intensity on complete complexation, [B] represents the DNA concentration in terms of total nucleotides and n is the number of nucleotides involved per molecule of the dye binding. Analyses of the fluorescence data following eqn (1) and considering ΔI_f^{∞} and K_{eq} as the fitting parameters provide the best fits to the data when n is assumed to be 2 (*cf.* insets in Fig. 1a and b). The K_{eq} values thus obtained for the AcH^+–DNA and Ac–DNA systems are 1.9×10^7 M^{-2} and 3.1×10^7 M^{-2}, respectively. The magnitudes of these K_{eq} values are very high and thus suggest extremely strong binding for both forms of the dye with DNA. Due to such strong binding with DNA, acridine dye is employed as a useful biological probe and also as a photoactivator towards DNA. It should be noted that similar high binding affinities have also been reported in the literature for other typical intercalator dyes with DNA.[41] About a 1.6-times higher binding constant for the Ac–DNA complex compared to the AcH^+–DNA complex indicates that the neutral form of the dye undergoes a relatively stronger binding with DNA than its protonated form. The result suggests that due to its neutral nature, the Ac undergoes a stronger intercalative mode of binding with DNA, through hydrophobic interaction, compared to AcH^+, for which electrostatic interaction would be the most likely binding mode.

The ground state absorption behaviour was also examined for both the AcH^+ and Ac forms of the dye in the presence of DNA. The absorption maximum for both forms of the dye appears at about 355 nm. The AcH^+ form is, however, distinctly characterized by its broad longer-wavelength shoulder absorption band spreading into the 380–440 nm region, which is absent for the neutral form of the dye.[19] Upon gradual addition of DNA to the AcH^+ and Ac solutions (at pH 4 and 8.5, respectively), the peak absorbance shows a gradual decrease along with small bathochromic shifts (~1 nm for AcH^+ and ~3 nm for Ac for the 354 nm band) and the appearance of isosbestic point-like features at ~360 nm for AcH^+ and ~392 nm for Ac (*cf.* Fig. S1 in the ESI†). These results are thus in corroboration with the SS fluorescence results presented in Fig. 1a and b suggesting a strong binding interaction for both prototropic forms of the dye with the DNA host.

The n value of 2 obtained from the analysis of the fluorescence titration data for both AcH^+–DNA and Ac–DNA systems indicates that there is simultaneous involvement of two nucleotides in the binding of a dye molecule to the DNA host. To verify such a stoichiometry further for the host–guest complexes in the AcH^+–DNA and Ac–DNA systems, we carried out Job's plot measurements[42,43] following both absorption and fluorescence studies. Fig. 2 shows the Job's plots for the AcH^+–DNA (pH 4) and Ac–DNA (pH 8.5) systems, respectively, obtained from

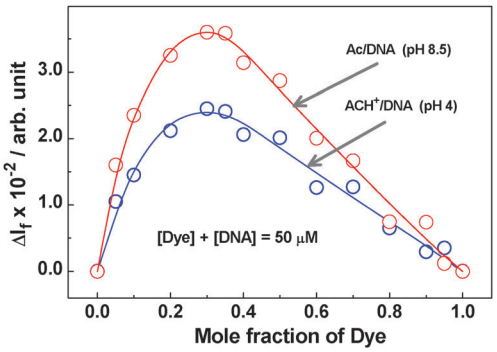

Fig. 2 Job's plots for the AcH^+–DNA (pH 4) and Ac–DNA (pH 8.5) systems obtained from fluorescence changes ($\Delta I_f = I_{dye-host} - I_{dye-only}$) as a function of the constituents. The sum of the dye and the host concentrations in these measurements was kept constant at 50 μM. The respective excitation and emission wavelengths were 360 nm and 482 nm for the AcH^+–DNA system, and 361 nm and 430 nm for the Ac–DNA system.

fluorescence measurements. The Job's plots for these systems as obtained from absorption measurements are shown in Fig. S2 in the ESI.† The maxima of these Job's plots appear at around a 0.33 mole fraction of the dye and thus unambiguously establish the 1 : 2 (dye to host) stoichiometry of the complexes formed in both the AcH^+–DNA and Ac–DNA systems.

Knowing about the strong interaction of the dye with DNA, we subsequently carried out absorption and SS fluorescence measurements to explore the interaction of the dye with the recognized drug carrier, HPβCD. For the Ac form of the dye (pH 8.5), there is a gradual decrease in the fluorescence intensity with an increase in the HPβCD concentration, along with the concomitant development of two new vibrational features in the spectra at ~427 and 445 nm and also a small hypsochromic shift in the emission maxima, as shown in Fig. 3. These results indicate formation of quite a strong inclusion complex for the Ac form of the dye with the HPβCD host. The hypsochromic shift and the development of vibrational features clearly suggest that the bound dye experiences a lower micropolarity on incorporation into the HPβCD cavity than in bulk water. Reduction in the fluorescence intensity for the Ac–HPβCD systems is justifiably

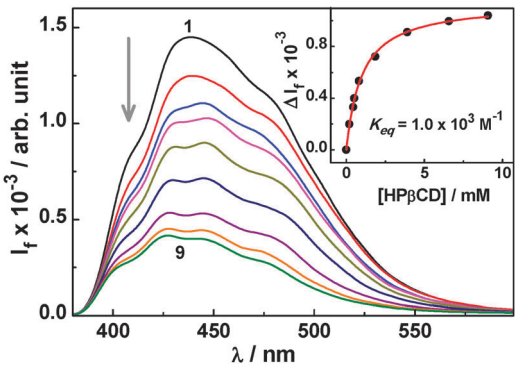

Fig. 3 Changes in the SS fluorescence spectra for the Ac–HPβCD system at pH 8.5; [Ac] = 13.6 μM and [HPβCD] = 0, 0.2, 0.43, 0.5, 0.81, 1.85, 3.9, 6.6, and 9.1 mM for spectra 1–9. Inset: fluorescence titration curve for the Ac–HPβCD system at pH 8.5, analysed using eqn (1) with n = 1.

Open Access Article. Published on 26 February 2015. Downloaded on 2/25/2026 10:40:43 AM.
This article is licensed under a Creative Commons Attribution 3.0 Unported Licence.

assigned to the strong hydrogen bonding interaction of the encapsulated Ac with the portal OH groups of the HPβCD host, as was also observed in our earlier study on the interaction of the dye with the unsubstituted βCD host.[19]

In accordance with the SS fluorescence results, in the absorption studies also there is a small decrease in the absorbance along with a small red shift (~2 nm) in the absorption maximum for the Ac form (pH 8.5) of the dye on addition of the HPβCD host in the solution (*cf.* Fig. S3a, ESI†). Observed results support a reasonable host–guest interaction in the Ac–HPβCD system. Unlike the neutral Ac form, the protonated AcH^+ form of the dye, however, did not show any appreciable change, either in the absorption (*cf.* Fig. S3b, ESI†) or in the fluorescence (*cf.* Fig. S4, ESI†) characteristics, on addition of the HPβCD host in the solution. These observations suggest that the interaction of the AcH^+ form of the dye with HPβCD host is extremely weak in comparison to that of the neutral Ac form of the dye.

A Job's plot study[42,43] was carried out for the Ac–HPβCD system at pH 8.5 to explore the stoichiometry of the complex formed in this case. Due to very small changes that occur in the absorbance of Ac on addition of the HPβCD host (*cf.* Fig. S3a, ESI†), no meaningful Job's plot could be obtained for the Ac–HPβCD system from absorption measurements. A satisfactory Job's plot for the present system, however, could be obtained from the fluorescence study, as shown in Fig. 4, indicating a maximum at around a 0.5 mole fraction of the dye and thus suggesting the 1 : 1 stoichiometry of the complex formed in this system. For the AcH^+–HPβCD (pH 4) system, as the interaction was found to be extremely weak from both absorption and fluorescence studies (*cf.* Fig. S3b and S4, ESI†), a Job's plot measurement was not attempted for this system.

A fluorescence titration method was utilized to evaluate the binding constant (K_{eq}) value for the Ac–HPβCD system. As shown in the inset of Fig. 3, the changes in the fluorescence intensity (ΔI_f) as a function of the host concentration fit well with the consideration of 1 : 1 complex formation (*cf.* eqn (1) with $n = 1$), as suggested from the Job's plot. The K_{eq} value thus estimated for the Ac–HPβCD complex is about 1.0×10^3 M^{-1}. It should be mentioned here that the binding interaction of Ac with HPβCD is about 3.4 times higher than that observed with the parent βCD host, reported in our earlier study.[19] It is thus evident that the extended cage structure offered by the HPβCD host renders a much greater hydrophobic interaction for the Ac form of the dye, leading to formation of a stronger inclusion complex. For the AcH^+ form of the dye, as there was no appreciable change either in the absorption or in fluorescence characteristics (*cf.* Fig. S3b and S4, ESI†), no titration study could be carried out for the AcH^+–HPβCD system to estimate the binding constant value.

1.1.2. ^{1}H NMR studies on the dye–host systems. To get an insight into the mode of binding in the present dye–host systems, the ^{1}H NMR measurements were carried out in D_2O solution. Fig. 5 shows the NMR spectra obtained for free Ac and the Ac–HPβCD system recorded at pD 8.5. As indicated from this figure, the NMR signals for all the aromatic protons of Ac undergo a small downfield shift on interaction with HPβCD. Since both ends of Ac along its long axis are equivalent, an axial incorporation of the dye into the HPβCD cavity can involve either of its axial ends equally. Therefore, the NMR signals for all the aromatic protons of Ac are expected to undergo very similar shifts, as we observe experimentally. It should be mentioned here that similar downfield shifts in the NMR signals for all the aromatic protons of Ac have also been reported in the literature for its interaction with the parent βCD host.[44] One interesting observation in the present NMR results for the Ac–HPβCD system is that the two NMR peaks at the middle of the apparent quartet associated with the H1 and H4 protons of Ac are almost merged with each other on interaction of the dye with the HPβCD host, a unique feature not observed earlier for the Ac–βCD system.[44] This is certainly due to different extent of shifts for the H1 and H4 proton signals on interaction of the dye with HPβCD, though exact details of these shifts could not be unraveled from the present study. For the AcH^+–HPβCD system (pH 4), since no appreciable dye–host interaction was indicated from absorption and fluorescence measurements (*cf.* Fig. S3a and S4, ESI†), no NMR study was attempted for this system.

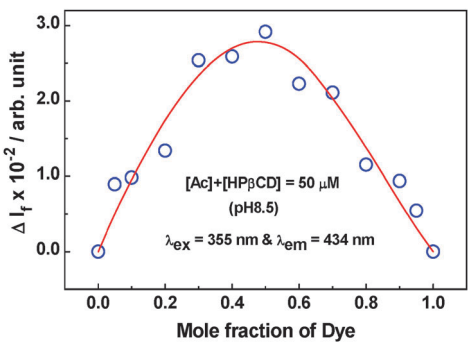

Fig. 4 Job's plot obtained for the Ac–HPβCD (pH 8.5) system using fluorescence measurement. The sum of the dye and the host concentrations in these measurements was kept constant at 50 μM. Excitation and emission wavelengths were 355 nm and 434 nm, respectively.

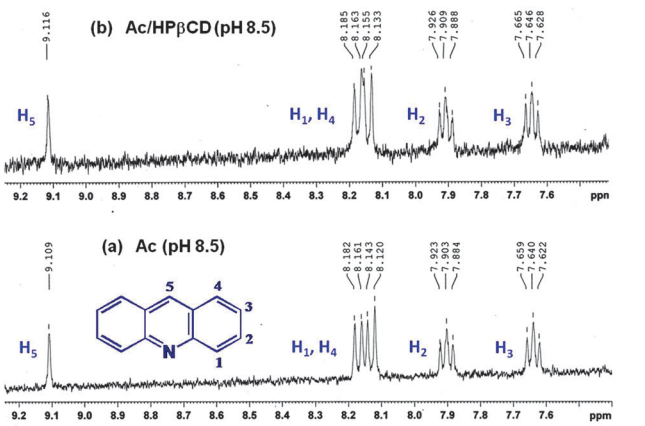

Fig. 5 ^{1}H NMR spectra of (a) free Ac and (b) the Ac–HPβCD system obtained at pH 8.5. Concentrations of the components were: [Ac] = 150 μM and [HPβCD] = 150 mM.

 This journal is © the Owner Societies 2015

Open Access Article. Published on 26 February 2015. Downloaded on 2/25/2026 10:40:43 AM.
This article is licensed under a Creative Commons Attribution 3.0 Unported Licence.

^{1}H NMR studies were also carried out for the Ac–DNA system in D_2O solution at pD 8.5. The NMR spectra recorded for the free Ac and the Ac–DNA system under similar experimental conditions are shown in Fig. S5 of the ESI.† As indicated from this figure, there are no distinguishable NMR signals for the Ac–DNA system that can be attributed either to the guest dye or to the DNA host (*cf.* Fig. S5b, ESI†), even though characteristic NMR signals are clearly observed for free dye in the absence of DNA under similar experimental conditions (*cf.* Fig. S5a, ESI†). As the DNA molecules possess a large number of exchangeable protons, it appears that in the present experimental conditions all the proton signals of DNA are exceedingly well-broadened causing the development of a significant background such that not only the DNA signals but also those of the guest dye are masked under this background. As the NMR results for the Ac–DNA system were not conclusive, a similar NMR study for the AcH^+–DNA system was not carried out in the present work.

1.1.3. Modulation of the prototropic equilibrium of the dye. Observing that the Ac and AcH^+ forms of the dye interact quite differently with both DNA and the HPβCD hosts, it was expected that the dye will display significant modulation of its acid–base property on interaction with these hosts. The prototropic equilibrium for the dye in the presence of DNA or the HPβCD hosts can be represented by a four-state dynamic equilibrium model as shown in Scheme 2, where K_a and K_a' represent the acid dissociation constants for the free and the bound dye and K_{eq} and K_{eq}' represent the binding constants for the Ac and AcH^+ forms of the dye with the host (H) used.

The modulation of the acid–base properties of the dye upon its interaction with DNA and HPβCD hosts was investigated systematically by following the pH-dependent changes in the absorption spectra of the dye in the presence of significantly high concentrations of the hosts, as shown in Fig. S6 of the ESI.† Absorbance changes were noted at selected wavelengths in the absence as well as in the presence of DNA and HPβCD hosts, separately, as a function of the pH of the solution, as shown in Fig. 6. The pK_a values were estimated from the inflection points of the plots and are found to be 5.4, 5.0 and 4.4 for the free dye, dye–DNA and dye–HPβCD systems, respectively.

As indicated by the observed results, the pK_a value of the dye undergoes about 0.4 and 1.0 units of downward shift on its interaction with DNA and the HPβCD hosts, respectively, which supports the preferential binding of the Ac form of the dye with both the DNA and HPβCD hosts compared to

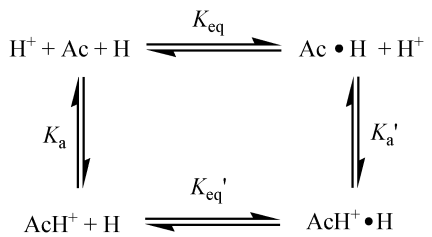

Scheme 2 Four-state thermodynamic equilibrium model for the acridine dye and host (H, either HPβCD or DNA) systems considering all the stages of host–guest interaction and the acid dissociation processes.

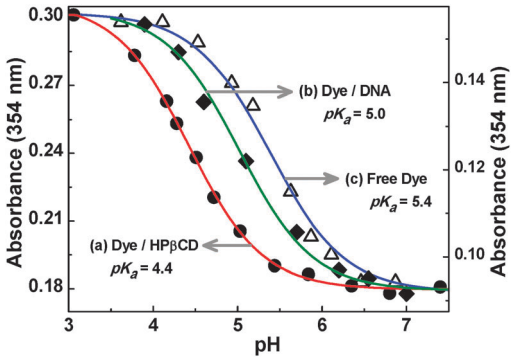

Fig. 6 Changes in the absorbance of acridine dye (10 μM) at 354 nm measured in the presence of (a) 30 mM HPβCD, (b) 800 μM DNA and (c) in the absence of any host, as a function of the pH of the solution.

the AcH^+ form, as inferred earlier from the fluorescence titration studies (*cf.* Section 1.1.1). The larger pK_a shift for the dye–HPβCD system (1.0 units) compared to that of the dye–DNA system (0.4 units) is directly in accordance with the observation that there is a larger difference in the binding affinities for the Ac and AcH^+ forms of the dye with HPβCD host than with DNA. Importantly, the difference in the pK_a shifts between the dye–DNA and dye–HPβCD systems can be exploited suitably to achieve a preferential binding for the dye, either to the DNA or to the HPβCD host, in a given dye–DNA–HPβCD ternary system, just by adjusting the pH of the solution, as discussed in the following sections.

1.2. Competitive interaction of acridine dye with HPβCD and DNA hosts at pH 5.5

Competitive binding interaction of the two prototropic forms of acridine dye has been investigated at pH 5.5, a characteristic pH of cancer cells, in the simultaneous presence of both DNA and HPβCD hosts. As expected, at this pH the absorption spectrum of the free dye (*cf.* Fig. 7) exhibits a broad absorption shoulder at the longer wavelength region (~400–440), an exclusive feature for the AcH^+ form of the dye, along with the absorption maximum at 354 nm. These observations are consistent with the pK_a value of 5.4 for the dye,[19] suggesting the presence of both AcH^+ and Ac forms of the dye in the solution at pH 5.5, both with significant proportions (almost 50 : 50).

Fig. 7a shows the changes in the absorption spectra of the dye with changing HPβCD concentration at pH 5.5. With an increase in HPβCD concentration, there is a decrease in the absorbance for both the 354 nm main band and the 400–440 nm shoulder band along with a small red shift in the main absorption band by ~3 nm. These changes are certainly due to the formation of the dye–HPβCD inclusion complex. Interestingly, it is observed from Fig. 7a that in the presence of HPβCD at pH 5.5 there is a relatively larger decrease in the absorbance for the 400–440 nm shoulder band in comparison to that of the 354 nm main band. This observation suggests that the relative proportion of the Ac form is enhanced in the solution upon increasing the HPβCD concentration, as a consequence of the downward pK_a shift of the dye due to preferential Ac–HPβCD complex formation.

Open Access Article. Published on 26 February 2015. Downloaded on 2/25/2026 10:40:43 AM.
This article is licensed under a Creative Commons Attribution 3.0 Unported Licence.

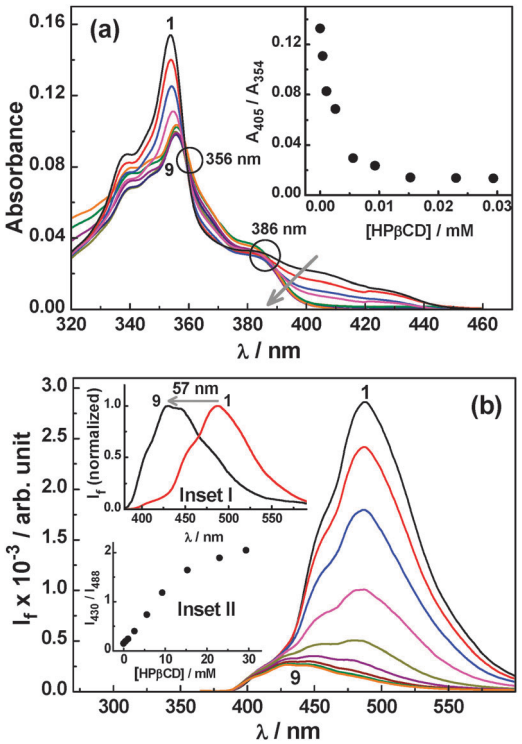

Fig. 7 (a) Changes in the absorption spectra for the Ac–HPβCD system at pH 5.5; [Ac] = 10 μM and [HPβCD] = 0, 0.46, 1.08, 2.6, 5.6, 9.3, 15.3, 23, and 29.4 mM for spectra 1–9. Inset: ratio of absorbance at 405 and 354 nm (A_{405}/A_{354}) as a function of HPβCD concentration. (b) Changes in the SS fluorescence spectra for the Ac–HPβCD system at pH 5.5; [Ac] = 10.6 μM and [HPβCD] = 0, 0.46, 1.08, 2.6, 5.6, 9.3, 15.3, 23, and 29.4 mM for spectra 1–9. Inset I: normalized fluorescence spectra for (1) only Ac and (9) Ac–HPβCD (29.4 mM) at pH 5.5. Inset II: ratio of fluorescence intensities at 430 and 488 nm (I_{430}/I_{488}) as a function of HPβCD concentration.

Appearance of the kind of isosbestic points at about 360 and 386 nm in the absorption spectra with increasing HPβCD concentration also supports the conversion of some of the AcH^+ to the Ac form through the preferential formation of the Ac–HPβCD complex. This is further indicated by the plot shown in the inset of Fig. 7a, displaying a sharp decrease in the ratio of absorbance at 405 nm (mainly due to AcH^+) to that at 354 nm (both AcH^+ and Ac contributes) with an increase in the HPβCD concentration.

Studies on the acridine dye–HPβCD system at pH 5.5 have also been carried out using SS fluorescence measurements and the results are shown in Fig. 7b. It is observed that upon increasing the HPβCD concentration there is a large decrease in the fluorescence intensity along with a large blue shift in the emission peak, as large as ~57 nm (*cf.* inset I of Fig. 7b). These results clearly manifest the switch over of a large fraction of the AcH^+ emission in the absence of HPβCD to the predominantly Ac emission in the presence of HPβCD, suggesting the host-assisted deprotonation of AcH^+ at the studied pH conditions. It is thus evident that, without changing the pH, one can change the proportions of the prototropic forms of the dye in the solution, just by the addition of the HPβCD host. Inset II of Fig. 7b, shows the plot of fluorescence intensity ratio (I_{430}/I_{488}) for the dye at 430 nm (Ac) to 488 nm (AcH^+), as a function of the increasing HPβCD concentration. As revealed from this plot, the intensity ratio increases sharply upon increasing the host concentration, indicating the preferential formation of the Ac–HPβCD inclusion complex in the system and thereby a shift in the overall prototropic equilibrium of the dye gradually towards the Ac form. The K_{eq} value for the Ac–HPβCD system was also estimated from fluorescence titration data at pH 5.5 (*cf.* Fig. S7a, ESI†) and is found to be 560 M^{-1}, half of the value estimated at pH 8.5. This reduction in the K_{eq} value arises because at pH 5.5 a fraction of dye remains in the protonated form which does not interact with HPβCD (*cf.* Section 1.1.1).

As discussed in Section 1.1, both HPβCD and DNA show greatly different binding affinities for the AcH^+ and Ac forms of the dye. Such a property can be exploited to control the binding of the dye preferentially to either the HPβCD or DNA hosts, simply by adjusting the pH of the solution. To realize such control and to achieve a possible dye relocalization from HPβCD to DNA, the photochemical changes for the dye (10 μM)/HPβCD (30 mM) system at pH 5.5 was further explored in the presence of varying DNA concentrations. Fig. 8a depicts the changes in the absorption spectra of the Ac–HPβCD system with changing

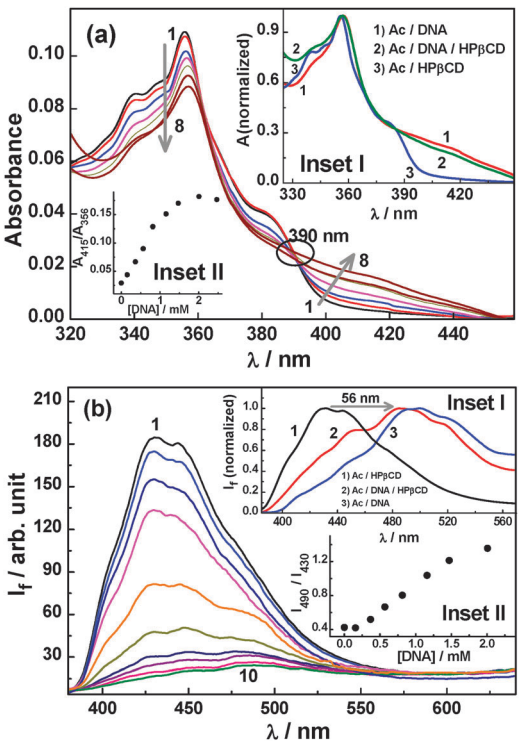

Fig. 8 (a) Changes in the absorption spectra for the Ac–HPβCD system upon addition of DNA at pH 5.5; [Ac] = 11 μM, [HPβCD] = 30 mM and [DNA] = 0, 0.16, 0.37, 0.57, 0.81, 1.16, 2.02, and 2.47 mM for spectra 1–8. Inset I: normalized absorption spectra for (1) Ac–DNA, (2) Ac–DNA–HPβCD and (3) Ac–HPβCD at pH 5.5; [Ac] = 11 μM, [HPβCD] = 30 mM and [DNA] = 2.47 mM. Inset II: ratio of absorbances at 415 and 356 nm with increasing DNA concentration. (b) Changes in the SS fluorescence spectra for the Ac–HPβCD system upon addition of DNA at pH 5.5; [Ac] = 11 μM, [HPβCD] = 30 mM and [DNA] = 0, 0.07, 0.16, 0.37, 0.57, 0.81, 1.16, 1.47, 2.02, and 2.47 mM for spectra 1–10. Inset I: normalized fluorescence spectra for (1) Ac–HPβCD, (2) Ac–DNA–HPβCD and (3) Ac–DNA at pH 5.5. [Ac] = 11 μM, [HPβCD] = 30 mM and DNA = 2.47 mM. Inset II: ratio of fluorescence intensities at 490 and 430 nm with increasing DNA concentration.

This journal is © the Owner Societies 2015

Open Access Article. Published on 26 February 2015. Downloaded on 2/25/2026 10:40:43 AM.
This article is licensed under a Creative Commons Attribution 3.0 Unported Licence.

DNA concentration. The results show an appreciable regain of the broad longer wavelength shoulder band of the AcH^+ form of the dye, implying that the dye slowly detaches from the Ac–HPβCD complex and subsequently binds to the DNA host through protonation of the detached dye. This is further evidenced from the appearance of the clear isosbestic point at ~390 nm. Formation of a good extent of the AcH^+–DNA complex is also supported by the comparison of the absorption spectra in the related binary and ternary systems (*cf.* inset I of Fig. 8a) and by the changes in the absorbance ratio of 415 nm to 356 nm for the ternary system (*cf.* inset II of Fig. 8a). The observed results clearly indicate that at pH 5.5, the dye prefers to bind to the DNA host over HPβCD through the formation of the AcH^+–DNA complex in lieu of the Ac–HPβCD complex. This is in accordance with the higher pK_a value (5.0) for the dye–DNA system as compared to that of the dye–HPβCD system (4.4).

The fluorescence spectral features of the Ac–HPβCD system at pH 5.5 also undergo large changes upon the addition of DNA, as shown in Fig. 8b. With an increase in the DNA concentration, the fluorescence intensity undergoes a large reduction, indicating the disruption of the dye–HPβCD complex in the presence of DNA. Additionally, the fluorescence peak at 430 nm slowly disappears and a prominent new peak appears at 487 nm, illustrating the substantial formation of the AcH^+–DNA complex in the system. In the present case, since the solution pH is close to the dye pK_a, a reasonable amount of the Ac–HPβCD and Ac–DNA complexes are present in the solution, as indicated by the small hump at around 450 nm for the Ac–DNA–HPβCD system (*cf.* inset I of Fig. 8b). Upon comparison of the fluorescence spectra for the relevant binary and ternary systems, as shown in the inset I of Fig. 8b, it is clearly exemplified that DNA dominates the binding of the dye at pH 5.5 compared to the HPβCD host. It is noticed from inset II of Fig. 8b that the fluorescence intensity ratio for the acridine dye between 490 and 430 nm (I_{490}/I_{430}) increases reasonably sharply with an increase in the DNA concentration. This observation is directly in corroboration with the fact that at pH 5.5 the dye shows a preferential binding towards DNA over HPβCD, resulting in a major fraction of the dye undergoing relocation from the HPβCD nanocavity to the DNA pocket. Thus, at pH 5.5, the HPβCD in effect plays the role of a drug transport vehicle, supplying the dye–drug for binding to the DNA target. The binding constant value for the formation of the new AcH^+–DNA complex in the presence of HPβCD was estimated following eqn (1) and is found to be $4.6 \times 10^6\ M^{-2}$, which is ~a quarter of the value estimated at pH 4 in the absence of HPβCD (Fig. S7b, ESI†). This is expected because there is a competition between DNA and HPβCD to bind the dye and hence the dye binding with DNA is significantly affected by the presence of HPβCD and *vice versa*. In the present case, the number of nucleotides (n) required to bind a dye is also found to be two (*cf.* Fig. S7b, ESI†), similar to that obtained in the absence of the HPβCD host at pH 4 and 8.5, suggesting that the HPβCD does not have any direct interaction with DNA such that the mode of dye binding to DNA remains unaltered. It should be noted here that in the literature it is also well-documented that there is hardly any interaction of cyclodextrin hosts with DNA.[45,46]

1.3. pH triggered delivery of acridine dye from HPβCD host to DNA

As binding interactions in the studied systems are noncovalent in nature, it is interesting to see if the dye binding and relocation between the HPβCD and DNA can be controlled at will using pH as a stimulus, which could eventually be exploited rationally in applications such as controlled drug delivery. Taking into consideration the pH range where denaturation of DNA does not take place (pH 4 to 9),[47–50] we systematically investigated the dye–HPβCD–DNA ternary system at two different pH conditions, namely pH 4 and 8.5, where acridine dye will exist mainly in the AcH^+ and Ac forms, respectively. Results of these studies are very intriguing and are described in the following sections.

1.3.1. Absorption and fluorescence studies. The absorption and fluorescence spectra of the dye in the dye–HPβCD–DNA ternary system at pH 8.5 are shown in Fig. 9a and b and those at pH 4 are shown in Fig. 10a and b, respectively. Absorption and fluorescence spectra for the dye in the dye–HPβCD, dye–DNA and dye alone cases at the respective pH conditions are also shown in the corresponding figures for comparison. As indicated from Fig. 9a and b, at pH 8.5, the normalized absorption and fluorescence spectra of the dye–HPβCD–DNA ternary system resembles quite closely those of the dye–HPβCD system, with a prominent absorption peak at 356 nm and dual emission peaks centred at 427 and 445 nm, indicating preferential binding of Ac to HPβCD in the dye–HPβCD–DNA ternary system. For Ac–DNA binding at pH 8.5, considering n equal to two and assuming that

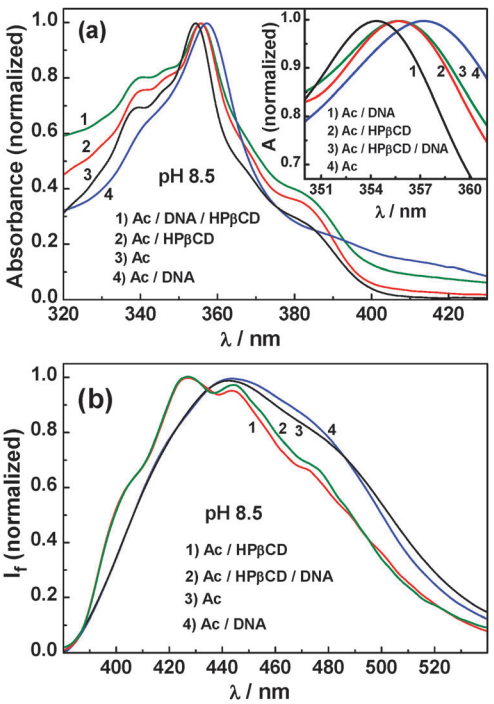

Fig. 9 (a) Normalized absorption spectra for the Ac–DNA–HPβCD, Ac–HPβCD, Ac and Ac–DNA systems at pH 8.5. [Ac] = 11 μM, [HPβCD] = 10 mM and DNA = 2.0 mM. (b) Normalized SS fluorescence spectra for the Ac–HPβCD, Ac–HPβCD–DNA, Ac and Ac–DNA systems at pH 8.5. [Ac] = 11 μM, [HPβCD] = 10 mM and DNA = 2.0 mM.

Open Access Article. Published on 26 February 2015. Downloaded on 2/25/2026 10:40:43 AM.
This article is licensed under a Creative Commons Attribution 3.0 Unported Licence.

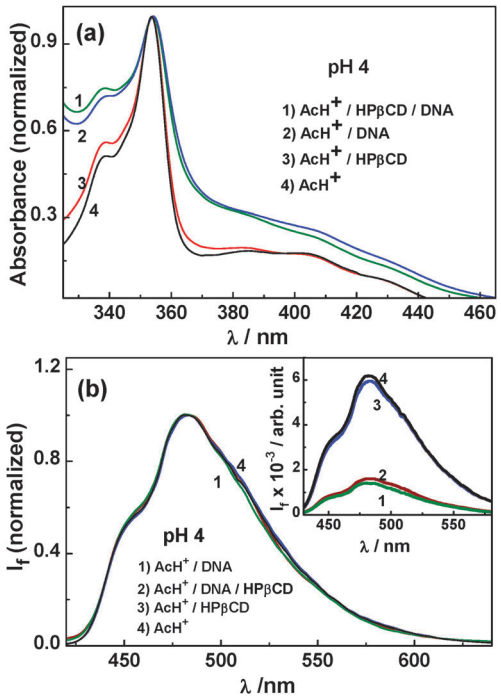

Fig. 10 . (a) Normalized absorption spectra for the AcH^+–DNA–HPβCD, AcH^+–DNA, AcH^+–HPβCD and AcH^+ systems at pH 4. [AcH^+] = 11 μM, [HPβCD] = 10 mM and DNA = 2.0 mM. (b) Normalized SS fluorescence spectra for the AcH^+–DNA, AcH^+–DNA–HPβCD, AcH^+–HPβCD and AcH^+ systems at pH 4. [AcH^+] = 11 μM, [HPβCD] = 10 mM and DNA = 2.0 mM.

all nucleotides have similar binding affinity toward Ac, the effective binding constant per nucleotide could be expressed as $\sqrt{3 \times 10^7\ M^{-2}}$, which is equal to $\sim 5 \times 10^3\ M^{-1}$. This value is about 5 times larger than the K_{eq} value for the Ac–HPβCD system ($\sim 1 \times 10^3\ M^{-1}$). Though the comparison of these binding constants suggests that the dye can reside better in DNA, the observed spectral features suggest that the dye is preferentially going into the HPβCD nanocavity under the present experimental conditions. The preferential binding of the dye to HPβCD is understandably assisted by about a five times higher concentration of HPβCD compared to DNA used in the solution. Thus, from the experimental results, it is very evident that in the dye–HPβCD–DNA ternary system at pH 8.5, the dye can be preferentially bound to the HPβCD cavity in its neutral form Ac, using a reasonably high concentration of the macrocyclic host and thereby resisting the binding of the dye to the DNA host.

As indicated from Fig. 10a and b, absorption and fluorescence spectral features of the dye–HPβCD–DNA ternary system at pH 4 match quite well with those of the dye–DNA system, signifying that the binding feature of the dye has now been tuned at this lower pH for preferential binding to the DNA pocket as the AcH^+ form of the dye. From the present results, it is clearly evident that HPβCD can be applied as a useful pH-sensitive delivery nano-vehicle for the supply of the dye–drug to target DNA for a programmed acidolysis. The fact that the HPβCD macrocycle shows negligible or no interaction with either the free AcH^+ or the AcH^+–DNA complex is also evidenced from the results shown in the inset of Fig. 10b where there is hardly any observable difference in the fluorescence spectra between the AcH^+ only and AcH^+–HPβCD systems and also between the AcH^+–DNA and AcH^+–DNA–HPβCD systems.

1.3.2. Circular dichroism measurements. It is known that valuable information on supramolecular host–guest complexes can be obtained from circular dichroism measurements.[51–53] In the present study, circular dichroism spectra were systematically recorded for the Ac–HPβCD, Ac–DNA and Ac–HPβCD–DNA systems at pH 8.5 and are shown in Fig. 11. Neither HPβCD nor DNA show any circular dichroism in the spectral region of the dye absorption. The free dye also shows no circular dichroism in the above spectral region. For the Ac–HPβCD system, however, there is a weak negative induced circular dichroism (ICD)[51–53] signal throughout the absorption band of the dye (*cf.* Fig. 11a), certainly arising due to the axial incorporation of the dye into the HPβCD cavity.[51–53] For the Ac–DNA system, there is a stronger positive ICD signal throughout the absorption band of the dye (*cf.* Fig. 11b). We attribute this strong ICD signal to the intercalation of dye into the DNA base pairs. Interestingly, for the Ac–HPβCD–DNA ternary system, the positive ICD signal (due to the Ac–DNA intercalative interaction) reduces drastically and a weak negative signal develops at the lower wavelength region of the spectra (*cf.* Fig. 11c), possibly due to the preferential formation of the Ac–HPβCD inclusion complex that displays a negative ICD signal (*cf.* Fig. 11a). Present results thus clearly indicate that at pH 8.5 the Ac form of the dye preferentially binds to the HPβCD host, possibly through the axial incorporation of the dye into the host cavity.[51–53]

Circular dichroism spectra were also recorded in this study for the AcH^+–HPβCD, AcH^+–DNA and AcH^+–HPβCD–DNA systems at pH 4 and the results are shown in Fig. S8 of the ESI.† As expected, the free AcH^+ did not show any circular dichroism. For the AcH^+–HPβCD system (*cf.* Fig. S8a, ESI†), there is also no observable ICD signal throughout the spectral region of the dye, suggesting no significant interaction of AcH^+ with the HPβCD host. For the AcH^+–DNA system, there is a positive ICD signal (*cf.* Fig. S8b, ESI†), albeit with much weaker intensity than that of the Ac–DNA system (*cf.* Fig. 11b), possibly suggesting that at pH 4 only a small

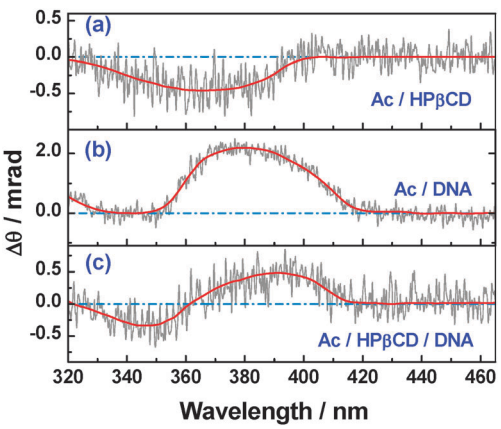

Fig. 11 Circular dichroism spectra of the (a) Ac–HPβCD, (b) Ac–DNA and (c) Ac–HPβCD–DNA systems (pH 8.5). Concentrations of the components were: [Ac] = 50 μM, [HPβCD] = 20 mM and [DNA] = 1.2 mM.

This journal is © the Owner Societies 2015

Open Access Article. Published on 26 February 2015. Downloaded on 2/25/2026 10:40:43 AM.
This article is licensed under a Creative Commons Attribution 3.0 Unported Licence.

fraction of the AcH^+ undergoes intercalative binding and results in the observed weak ICD signal while the majority of the AcH^+ undergoes electrostatic binding to the phosphate backbone of DNA and does not contribute to the ICD signal. For the AcH^+–HPβCD–DNA ternary system, the ICD spectrum (*cf.* Fig. S8c, ESI†) is quite similar to that of the AcH^+–DNA system (*cf.* Fig. S8b, ESI†), suggesting that at pH 4 the AcH^+ form of the dye remains almost exclusively bound to DNA even in the presence of a significantly high concentration of the HPβCD host.

1.3.3. Time-resolved fluorescence studies. Time-resolved (TR) fluorescence is a sensitive technique to characterize multiple emissive species present in a system. TR fluorescence studies were therefore carried out on the present dye–host systems to obtain more insight into the complexation processes, especially the pH-responsive selection of acridine dye by the HPβCD or DNA hosts. The excited-state lifetimes of AcH^+ and Ac as estimated following TR fluorescence studies at pH 4 and 8.5 (decays were single exponential at both of the pH conditions; *cf.* Fig. 12a and b, respectively) are 32 ns and 9.83 ns, respectively, very similar to the values reported in the literature.[36,37] Fluorescence decays for the dye in the presence of DNA, HPβCD and a DNA–HPβCD mixture at pH 4 and 8.5 are displayed in Fig. 12a and b, respectively. In these cases, the decays are either bi- or tri-exponential in nature. Different fluorescence decay parameters as obtained for these systems are listed in Table 1.

For the dye–DNA system at pH 4, the decay is bi-exponential in nature (*cf.* Fig. 12a). In this case, the longer lifetime component

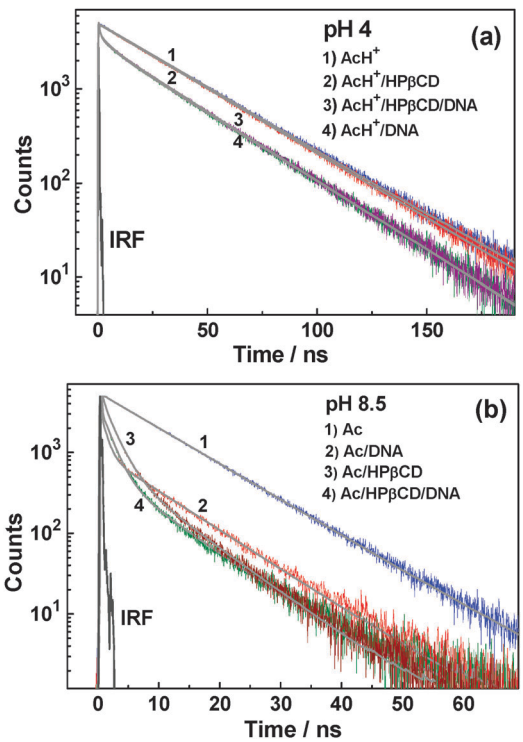

Fig. 12 (a) Fluorescence decay measured at 490 nm for the AcH^+, AcH^+–HPβCD, AcH^+–HPβCD–DNA and AcH^+–DNA systems at pH 4. [AcH^+] = 11 μM, [HPβCD] = 10 mM and DNA = 2.0 mM. (b) Fluorescence decay measured at 410 nm for the Ac, Ac–DNA, Ac–HPβCD and Ac–HPβCD–DNA systems at pH 8.5. [Ac] = 11 μM, [HPβCD] = 10 mM and DNA = 2.0 mM. IRF represents the instrument response function.

Table 1 Fluorescence decay parameters for (1) dye only, (2) dye–DNA, (3) dye–HPβCD and (4) dye–HPβCD–DNA at pH 4 and 8.5. The excitation wavelength was 374 nm and emission wavelengths were 485 nm at pH 4 and 410 nm at pH 8.5, respectively

System	pH	A_1 (%)	τ_1[a] (ns)	A_2 (%)	τ_2[a] (ns)	A_3 (%)	τ_3[a] (ns)
AcH^+	4	100	32.0				
AcH^+–DNA	4	96	29.0	4	1.52		
AcH^+–HPβCD	4	100	31.4				
AcH^+–HPβCD–DNA	4	96.5	28.9	3.5	1.6		
Ac	8.5	100	9.83				
Ac–DNA	8.5	79	8.65	21	0.48		
Ac–HPβCD	8.5	46	8.95	54	2.27		
Ac–HPβCD–DNA	8.5	34	8.6	52	2.27 (fixed)[b]	14	0.48 (fixed)[b]

[a] The error limit in the lifetime values is about 5%. [b] These shorter lifetime components needed to be fixed for consistency with the proposed model and to obtain a good fit to the observed decays.

($\tau_1 \sim 29$ ns) is marginally shorter than that of the free dye ($\sim$32 ns) and is attributed to the electrostatic binding (exo- or semi-intercalative binding) of AcH^+ to DNA. The shorter lifetime component ($\tau_2 \sim 1.52$ ns), which is drastically shorter than that of the free dye and shows only a small contribution to the overall decay is understandably due to the fraction of the AcH^+ intercalated between the DNA bases.[33,54] The observation that the contribution of the longer lifetime component is very high ($a_1 \sim 96\%$) in the present case suggests that at acidic pH the major fraction of the AcH^+ undergoes exo- or semi-intercalative binding to DNA, due to the strong electrostatic interaction between the cationic dye and the negative phosphate groups of the DNA backbone. Such an inference is also supported by the results obtained from the circular dichroism studies, discussed in Section 1.3.2, and the TR fluorescence anisotropy studies, discussed in the next section. The reduction in the fluorescence lifetime compared to that of the free dye is regarded to be due to a quenching process caused by the nucleobases, possibly through a photoinduced electron transfer interaction,[33,54–56] which is understandably very strong for the intercalated dye compared to the externally-bound dye.

Fluorescence decay for the dye–DNA system at pH 8.5 (*cf.* Fig. 12b) is also bi-exponential in nature, with a longer lifetime component ($\tau_1 \sim 8.65$ ns) that is marginally shorter and a shorter lifetime component ($\tau_2 \sim 0.48$ ns) that is drastically shorter than that of the free dye ($\sim$9.83 ns). Since no appreciable electrostatic interaction is expected for the neutral Ac form of the dye with DNA, we anticipate that shorter and longer lifetime components at pH 8.5 correspond to the intercalated and the free dyes, respectively, for which supporting evidence is obtained from the fluorescence anisotropy results discussed in the next section. It should be mentioned here that for both AcH^+ and Ac, the percentage reduction in the fluorescence lifetime due to DNA intercalation is very similar, about 94–95% compared to that of the free dye. Therefore, the observation that the shorter lifetime component has a greater contribution at pH 8.5 (21%) than at pH 4 (4%) suggests that the intercalation of the neutral Ac form of the dye into DNA is at least

Open Access Article. Published on 26 February 2015. Downloaded on 2/25/2026 10:40:43 AM.
This article is licensed under a Creative Commons Attribution 3.0 Unported Licence.

five times more favoured than that of the protonated AcH^+ form of the dye.

For the dye–HPβCD system, the fluorescence decay also exhibits a bi-exponential nature at pH 8.5 (*cf.* Fig. 12b). The shorter lifetime component ($\tau_2 \sim 2.27$ ns) is justifiably assigned to Ac encapsulated into the HPβCD cavity where a large reduction in the fluorescence lifetime compared to that of free Ac (~9.83 ns) arises due to strong fluorescence quenching caused by the H-bonding interaction of the bound dye with the portal OH groups of the HPβCD host.[19] The longer lifetime component ($\tau_1 \sim 8.95$ ns), which is just marginally shorter than that of the solution with the dye alone (~9.83 ns) is suggested to be due to the small fraction of the free dye that undergoes a dynamic fluorescence quenching by the HPβCD host, possibly involving a similar hydrogen bonding interaction. It should be mentioned that a similar quenching interaction for acridine dye has already been reported in our earlier study involving a parent βCD host.[19]

Interestingly, the fluorescence decay for the Ac–HPβCD–DNA ternary system at pH 8.5 resembles quite closely that of the Ac–HPβCD system but differs very greatly from that of the Ac–DNA system (*cf.* Fig. 12b). It is thus evident from the comparison of the fluorescence decays that in mildly basic solution, the Ac form of the dye in the Ac–HPβCD–DNA ternary system can be made to bind preferentially to the HPβCD host, even in the presence of a substantial concentration of DNA. In the present case, since multiple emissive species are present in the solution (*cf.* Table 1), the decay trace understandably required at least a tri-exponential function to fit acceptably and to be consistent with the proposed model, where the two shorter lifetime components correspond to the dye–DNA ($\tau_2 = 0.48$ ns) and dye–HPβCD complexes ($\tau_3 = 2.27$ ns) and the longer lifetime component ($\tau_1 = 8.6$ ns) represents the fraction of the free dye that undergoes dynamic quenching jointly by the HPβCD and DNA hosts present in the solution.

Fluorescence decays for the dye at different dye–host combinations at pH 4 are shown in Fig. 12a. As already mentioned, at pH 4 the fluorescence decay of the dye in the absence of any host is single-exponential in nature, with a lifetime of about 32 ns. For the dye–HPβCD system at pH 4, the decay interestingly shows a single-exponential nature, with only a small but quite systematic reduction in the lifetime with an increase in the HPβCD concentration. This observation suggests that the AcH^+ form does not undergo any appreciable inclusion complex formation but the free excited dye undergoes dynamic quenching to a small extent by the HPβCD host. An important observation to be noted from Fig. 12a is that the decay for the AcH^+–DNA–HPβCD ternary system exactly superimposes upon that of the AcH^+–DNA system, confirming that at acidic pH the dye is completely bound to the DNA host as its AcH^+ form. The observed TR fluorescence results are thus in complete correspondence with the results obtained from the ground state absorption and SS fluorescence studies, clearly indicating that in the dye–HPβCD–DNA ternary system the HPβCD in effect acts as a receptor to bind and stabilize the dye at higher pH and renders a complete relocation of the dye to the desired DNA target just upon reduction of the pH of the solution to the acidic region. In other words, HPβCD acts as an efficient nano-transporter to carry the dye–drug to the target DNA and delivers the model drug to the target upon using the drop in pH as the stimulus.

1.3.4. Fluorescence anisotropy studies. Fluorescence anisotropy decays for acridine dye were measured at pH 4 and 8.5, both in the absence and in the presence of DNA, HPβCD and a DNA–HPβCD mixture. The observed anisotropy decays for different systems at pH 4 and 8.5 are presented in Fig. 13a and b, respectively. Analysis of these decays required either mono-exponential or bi-exponential functions to obtain satisfactory fits. The anisotropy decay parameters obtained for the dye in different experimental conditions are listed in Table 2.

As expected, the anisotropy decays for the free dye are very fast and follow mono-exponential kinetics both at pH 4 and 8.5,

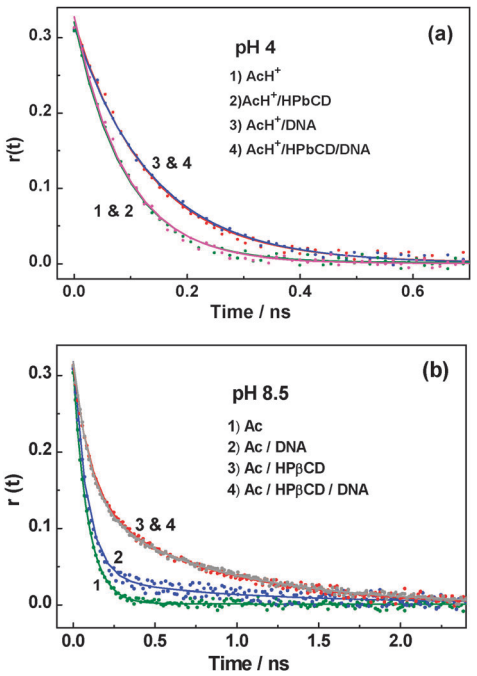

Fig. 13 (a) Time-resolved anisotropy decay curves for the AcH^+, AcH^+–HPβCD, AcH^+–HPβCD–DNA and AcH^+–DNA systems at pH 4. (b) Time-resolved anisotropy decay curves for the Ac, Ac–DNA, Ac–HPβCD and Ac–HPβCD–DNA systems at pH 8.5.

Table 2 Fluorescence anisotropy decay parameters for (1) dye only, (2) dye–DNA, (3) dye–HPβCD and (4) dye–HPβCD–DNA at pH 4 and 8.5. The excitation wavelength was 374 nm and the emission wavelengths were 485 nm at pH 4 and 410 nm at pH 8.5 respectively

System	pH	$r_{1,0}$	τ_{r1}[a] (ps)	$r_{1,0}$	τ_{r2}[a] (ps)
AcH^+	4	0.32	90		
AcH^+–HPβCD	4	0.32	91		
AcH^+–DNA	4	0.31	138		
AcH^+–HPβCD–DNA	4	0.32	133		
Ac	8.5	0.31	89		
Ac–HPβCD	8.5	0.17	95	0.14	760
Ac–DNA	8.5	0.28	89	0.03	910
Ac–HPβCD–DNA	8.5	0.18	96	0.14	770

[a] The error limit in the lifetime values is about 5%.

This journal is © the Owner Societies 2015

Open Access Article. Published on 26 February 2015. Downloaded on 2/25/2026 10:40:43 AM.
This article is licensed under a Creative Commons Attribution 3.0 Unported Licence.

giving rotational time constants (τ_{r1}) of about ~90 ps for both the AcH^+ (pH 4) and Ac (pH 8.5) forms of the dye. At pH 4, the decay for the AcH^+–HPβCD system also follows mono-exponential kinetics and gives a τ_{r1} value (~90 ps) very similar to that of the free AcH^+. It is thus evident that there is no appreciable interaction of AcH^+ with the HPβCD host, as also inferred from the SS and TR fluorescence and the circular dichroism results. Contrary to the AcH^+–HPβCD system, for the AcH^+–DNA system at pH 4, the anisotropy decay is slower and fits well with a mono-exponential function giving a τ_{r1} value (~140 ps) significantly higher than that of the free dye, although the increase is not exceedingly large. Recalling the TR fluorescence results in Table 1, it was indicated that in the AcH^+–DNA system at pH 4 there is a longer lifetime component τ_1 that shows the largest contribution (~96%) and was attributed to the AcH^+ exo-bound with DNA, while the shorter lifetime component τ_2, showing only a small contribution (~4%), was ascribed to the AcH^+ intercalatively-bound to DNA. In accordance with these TR fluorescence results, it is expected that the anisotropy decay for the AcH^+–DNA system at pH 4 is mainly due to the exo-bound AcH^+ and hence should effectively follow a mono-exponential function.[57] Since the AcH^+ exo-bound with DNA is expected to suffer only a small retardation in its rotational motion, the τ_{r1} value for the present system is accordingly increased only to a small extent compared to that of the free dye.

At pH 8.5, for both the Ac–HPβCD and Ac–DNA systems, the anisotropy decays follow bi-exponential kinetics. In both the cases, the τ_{r1} component is very similar to that of the free dye while the τ_{r2} component is drastically higher in comparison to τ_{r1}. As observed in the TR fluorescence studies (*cf.* Table 1), for the present systems the fluorescence decays are dominated by a longer lifetime component τ_1 attributed to the fraction of the free dye present in the solution. The observation that the τ_{r1} component for both the Ac–HPβCD and Ac–DNA systems resembles that of the free dye thus directly supports the proposition made from the TR fluorescence results. That the τ_{r2} component for both the dye–HPβCD and dye–DNA systems is much higher than τ_{r1} clearly suggests that this component is due to the Ac bound to the respective hosts, *via* inclusion complex formation with the HPβCD cavity and through intercalative binding to the DNA host. This is further supported by the fact that the τ_{r2} value for the Ac–DNA system is much higher than that of the Ac–HPβCD system, understandably because the rotational motion of the dye intercalatively-bound to DNA will be much more restricted in comparison to that of the dye incorporated into the HPβCD cavity. Further, from the comparison of the τ_{r2} value (910 ps) for the Ac–DNA system at pH 8.5 with the τ_{r1} value (140 ps) for the AcH^+–DNA system at pH 4 it is evident that the rotational motion of the DNA-bound Ac form is much more retarded than that of the DNA-bound AcH^+ form of the dye. This is in direct support of our inference that in the AcH^+–DNA system at pH 4, the cationic AcH^+ form of the dye mainly undergoes an exo-binding to DNA through an electrostatic interaction whereas in the Ac–DNA system at pH 8.5 the neutral Ac form of the dye mainly undergoes an intercalative mode of binding with the DNA host. For the dye–HPβCD system at pH 8.5, the longer τ_{r2} component is certainly due to the inclusion of Ac into the HPβCD cavity, which causes a large increase in the hydrodynamic volume of the fluorophore and hence an increase in the rotational time constant.

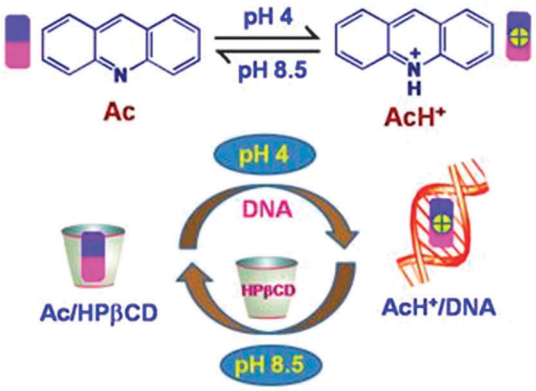

Scheme 3 Schematic representation of the pH-induced transfer of acridine from HPβCD to DNA at acidic pH and *vice versa*.

For the Ac–HPβCD–DNA ternary system at pH 8.5, the estimated anisotropy decay parameters (*cf.* Table 2 and Fig. 13b), match quite closely with those obtained for the Ac–HPβCD system. These results strongly support our proposition that in the Ac–HPβCD–DNA ternary system at pH 8.5 a major fraction of the Ac actually remained bound to the HPβCD cavity, even in the presence of a significantly high concentration of DNA. On the contrary, at acidic pH, the anisotropy decay for the AcH^+–HPβCD–DNA ternary system interestingly resembles quite closely with that of the AcH^+–DNA system (*cf.* Fig. 13a and Table 2). This observation directly reinstates the fact that at acidic pH the AcH^+ form of the dye almost exclusively binds to the DNA host, even in the presence of a substantially high HPβCD concentration. Thus, the observed results in effect suggest that, depending upon the pH of the solution, the HPβCD host not only selectively binds but also releases the active dye to the target DNA site, induced by a suitable pH change.

In brief, the fluorescence anisotropy results correspond very nicely with the ground state absorption and the SS and TR fluorescence results and establish the fact that reduction in the pH of the solution can provide a simple stimulus to quantitatively release the dye from the HPβCD cavity for its binding to the target DNA in a dye–HPβCD–DNA ternary system. Such a strategy of controlled dye–drug release mechanism can be easily visualized by the schematic presentation shown in Scheme 3. From the present model study it is evident that the HPβCD nanocarrier can effectively be used for controlled and targeted release of potential anticancer prodrugs under acidic conditions and thereby to selectively increase the local drug concentration at the targeted site, reducing the untoward side effect of the drug, an advantage that is highly desired in chemotherapeutic applications.

Conclusions

Interaction of an anticancer-active acridine dye with HPβCD, DNA and a HPβCD–DNA mixture has been investigated, using ground state absorption, steady-state fluorescence, time-resolved

Open Access Article. Published on 26 February 2015. Downloaded on 2/25/2026 10:40:43 AM.
This article is licensed under a Creative Commons Attribution 3.0 Unported Licence.

fluorescence, fluorescence anisotropy decay, ^{1}H NMR and circular dichroism measurements at different pH conditions. Results show that HPβCD selectively and strongly encapsulates the neutral dye Ac but shows almost no affinity for the protonated dye AcH^+. On the contrary, DNA interacts strongly with both the AcH^+ and Ac forms of the dye, albeit with a somewhat higher affinity for the Ac form. Consequently, the differential binding of the two prototropic forms of the acridine dye observed with the HPβCD and DNA hosts leads to about 1.0 units of downwards pK_a shift for the dye–HPβCD system and about 0.4 units of downwards pK_a shift for the dye–DNA system. Using the acridine dye–HPβCD–DNA ternary system as a model, we demonstrate in this study the interesting strategy of pH-dependent formation and dissociation of the dye–HPβCD complex, for a targeted and controlled release of the dye from the nanocavity of the biocompatible model drug carrier HPβCD to the target DNA site. In the dye–HPβCD–DNA ternary supramolecular system, HPβCD not only selectively binds and stabilizes the neutral Ac form of the dye at mildly alkaline pH but also explicitly delivers the active protonated AcH^+ form of the dye to the target DNA, triggered by a decrease in the pH to mildly acidic conditions. Thus, HPβCD acts as a model drug delivery agent to carry the dye to the target acceptor DNA. The potential of this unique supramolecular assembly may be explored in real biological systems where acidolysis can be used as a trigger for the controlled dissociation of the prodrug from the HPβCD inclusion complexes, leading to the association of the active form of the drug to the target site, such as to tumour cells or at the acidic organelles region, making the dye–drug more effective for the desired activity, with maximum selectivity. This model study would be very beneficial in relation to chemotherapeutic applications, nanoreactors, pharmaceutical development and can also be useful in designing new and promising stimuli-responsive assemblies for different biomedical applications. Future studies aim to investigate more into the interaction of anticancer acridine drugs with potential cyclodextrin derivatives for real pH-responsive biomedical applications.

Experimental section

Acridine dye (purity >99%) was obtained from Sigma-Aldrich, USA, and purified by re-crystallization from cyclohexane solution. Hydroxypropyl-β-cyclodextrin (HPβCD, *cf.* Scheme 1; average degree of substitution = 0.8, average MW = 1500) was purchased from Aldrich and used as received. Calf thymus DNA (ct-DNA) was purchased from Sigma and used as received. Nanopure water (Barnstead System; conductivity of 0.1 μS cm^{-1}) was used for all solution preparations. The dye solution was prepared by directly dissolving the dye sample and estimating its concentration from absorption spectral measurement (extinction coefficient 17 793 M^{-1} cm^{-1} at λ_{max} 355 nm for AcH^+ and 9700 M^{-1} cm^{-1} at λ_{max} 355 nm for Ac).[19] A known weight of HPβCD was directly added to the experimental solution to achieve the required host concentration. Stock ct-DNA solution was prepared by dissolving the solid DNA sample in nanopure water and keeping the solution stored overnight at 4 °C. Each time fresh DNA solution was prepared to perform the experiments. As ct-DNA has quite a large distribution in molecular sizes (8.0–15 kb), the concentration of DNA in the experimental solution was determined in terms of total nucleotide concentration, following absorbance at 260 nm and using an extinction coefficient of 6600 M^{-1} cm^{-1}.[58–60] That the DNA sample is free from protein impurities was ensured by observing the ratio of absorbance at 260 nm to that at 280 nm to be in the range of 1.8–1.9.[58–60]

All the measurements were carried out in aqueous solutions at suitable pH conditions at ambient temperature (~25 °C). The pH of the solutions was adjusted by adding dilute perchloric acid or dilute sodium hydroxide in small steps and the pH was measured using a pH meter (CL/46, Toshcon, India). Ground state absorption spectra and steady-state fluorescence spectra were recorded using a Jasco UV-visible spectrophotometer (model V-650; Tokyo, Japan) and a Hitachi spectrofluorimeter (model F-4500; Tokyo, Japan), respectively. Time-resolved fluorescence measurements were carried out using a time-correlated single-photon-counting (TCSPC) spectrometer,[57,61] obtained from IBH, UK. In these measurements, a 374 nm diode laser (pulse width ~100 ps, repetition rate 1 MHz) was used as the excitation source and a special photomultiplier tube (PMT)-based detection module supplied by Horiba Jobin Yvon IBH was used for the fluorescence detection. The instrument response function (IRF) for the TCSPC setup was measured using scattered light from a TiO_2 suspension in water and the full width half maximum (FWHM) of the IRF was found to be ~120 ps. All the measurements were carried out at a magic angle configuration to eliminate the effect of rotational anisotropy on the observed fluorescence decays. Observed decays were in general analyzed as a sum of exponentials (*cf.* eqn (2)), following a reconvolution procedure.[57,61]

$$I(t) = \sum B_i \exp(-t/\tau_i) \quad (2)$$

where B_i and τ_i are the pre-exponential factor and fluorescence lifetime, respectively, for the ith decay component. The quality of the fits and consequently the exponentiality of the decays were judged from the reduced chi-squared (χ^2) values and the distribution of the weighted residuals among the data channels.[57,61] For time resolved fluorescence anisotropy measurements, the fluorescence decays, $I_{\parallel}(t)$ and $I_{\perp}(t)$, corresponding to the parallel and perpendicular emission polarizations, respectively, with respect to the vertically polarized excitation light, were first measured. These decays were used to construct the anisotropy decay function $r(t)$:[57,61]

$$r(t) = \frac{I_{\parallel}(t) - GI_{\perp}(t)}{I_{\parallel}(t) + 2GI_{\perp}(t)} \quad (3)$$

where G is the correction factor for the polarization bias of the detection setup. The value of G was obtained independently by measuring two perpendicularly-polarized fluorescence decays while the sample was excited with the horizontally-polarized excitation light.[57,61] The ^{1}H NMR measurements were carried out using a Bruker 600 MHz NMR spectrometer. In the present measurements, the required solutions (~150 μM of dye and HPβCD each and 300 μM of DNA) were prepared in D_2O (99.8%) solvent. Required pD of the solutions were adjusted by adding

Open Access Article. Published on 26 February 2015. Downloaded on 2/25/2026 10:40:43 AM.
This article is licensed under a Creative Commons Attribution 3.0 Unported Licence.

dilute NaOD and DCl solutions in small steps and measured using the pH meter. The circular dichroism spectra were recorded using a UV-vis spectrophotometer/polarimeter model MOS-450 from Biologic Science Instruments, France.

Acknowledgements

The authors are thankful to Dr A. Barik of RPCD and Dr S. Dey of Chemistry Division, BARC, for their help in the circular dichroism and NMR measurements, respectively. The authors also thankfully acknowledge the Bhabha Atomic Research Centre, Mumbai, India, for the generous support provided during the course of the present research work.

Notes and references

1 R. L. Carrier, L. A. Miller and I. Ahmed, *J. Controlled Release*, 2007, **123**, 78–99.
2 K. Uekama, F. Hirayama and T. Irie, *Chem. Rev.*, 1998, **98**, 2045–2076.
3 D. W. Kuykendall and S. C. Zimmerman, *Nat. Nanotechnol.*, 2007, **2**, 201–202.
4 G. Astray, C. Gonzalez-Barreiro, J. C. Mejuto, R. Rial-Otero and J. Simal-Gandara, *Food Hydrocolloids*, 2009, **23**, 1631–1640.
5 Z. Qi and C. A. Schalley, *Acc. Chem. Res.*, 2014, **47**, 2222–2233.
6 M. D. Pluth, R. G. Bergman and K. N. Raymond, *Science*, 2007, **316**, 85–88.
7 E. M. M. D. Valle, *Process Biochem.*, 2004, **39**, 1033–1046.
8 K. Langa, J. Mosinger and D. M. Wagnerová, *Coord. Chem. Rev.*, 2004, **248**, 321–350.
9 H. Yamaguchi, T. Ogoshi and A. Harada, Sensor Development Using Existing Scaffolds, in *Chemosensors: Principles, Strategies, and Applications*, ed. B. Wang and E. V. Anslyn, John Wiley & Sons, New Jersey, 2011, ch. 11, pp. 211–226.
10 M. Shaikh, S. D. Choudhury, J. Mohanty, A. C. Bhasikuttan, W. M. Nau and H. Pal, *Chem. – Eur. J.*, 2009, **15**, 12362–12370.
11 M. Shaikh, J. Mohanty, A. C. Bhasikuttan, V. D. Uzunova, W. M. Nau and H. Pal, *Chem. Commun.*, 2008, 3681–3683.
12 G. Chen and M. Jiang, *Chem. Soc. Rev.*, 2011, **40**, 2254–2266.
13 J. Zhang and P. X. Ma, *Adv. Drug Delivery Rev.*, 2013, **65**, 1215–1233.
14 I. Ghosh and W. M. Nau, *Adv. Drug Delivery Rev.*, 2012, **64**, 764–783.
15 Y. Cao, X. Hu, Y. Li, X. Zou, S. Xiong, C. Lin, Y. Shen and L. Wang, *J. Am. Chem. Soc.*, 2014, **136**, 10762–10769.
16 V. T. Perchyonok and T. Oberholzer, *Curr. Org. Chem.*, 2012, **16**, 2365–2378.
17 T. Loftsson and D. Duchene, *Int. J. Pharm.*, 2007, **329**, 1–11.
18 W. Al-Soufi, B. Reija, M. Novo, S. Felekyan, R. Kuhnemuth and C. A. M. Seidel, *J. Am. Chem. Soc.*, 2005, **127**, 8775–8784.
19 M. Shaikh, Y. M. Swamy and H. Pal, *J. Photochem. Photobiol., A*, 2013, **258**, 41–50.
20 M. Shaikh, J. Mohanty, P. K. Singh, W. M. Nau and H. Pal, *Photochem. Photobiol. Sci.*, 2008, **7**, 408–414.
21 V. Khorwal, B. Sadhu, A. Dey, M. Sundararajan and A. Datta, *J. Phys. Chem. B*, 2013, **117**, 8603–8610.
22 S. Gould and R. C. Scott, *Food Chem. Toxicol.*, 2005, **43**, 1451–1459.
23 Z. Huang, S. Tian, X. Ge, J. Zhang, S. Li, M. Li, J. Cheng and H. Zheng, *Carbohydr. Polym.*, 2014, **107**, 241–246.
24 K. Miyake, H. Arima, F. Hirayama, M. Yamamoto, T. Horikawa, H. Sumiyoshi, S. Noda and K. Uekama, *Pharm. Dev. Technol.*, 2000, **5**, 399–407.
25 C. Liu, Z. Jiang, Y. Zhang, Z. Wang, X. Zhang, F. Feng and S. Wang, *Langmuir*, 2007, **23**, 9140–9142.
26 A. Rescifina, C. Zagni, M. G. Varrica, V. Pistarà and A. Corsaro, *Eur. J. Med. Chem.*, 2014, **74**, 95–115.
27 S. Monti and I. Manet, *Chem. Soc. Rev.*, 2014, **43**, 4051–4067.
28 X. Chen, L. Chen, X. Yao, Z. Zhang, C. He, J. Zhang and X. Chen, *Chem. Commun.*, 2014, **50**, 3789–3791.
29 A. Rajendran and B. U. Nair, *Biochim. Biophys. Acta*, 2006, **1760**, 1794–1801.
30 P. Belmont, J. Bosson, T. Godet and M. Tiano, *Anti-Cancer Agents Med. Chem.*, 2007, **7**, 139–169.
31 A. J. Pickard, F. Liu, T. F. Bartenstein, L. G. Haines, K. E. Levine, G. L. Kucera and U. Bierbach, *Chem. – Eur. J.*, 2014, **20**, 1–15.
32 F. Charmantray, M. Demeunynck, D. Carrez, A. Croisy, A. Lansiaux, C. Bailly and P. Colson, *J. Med. Chem.*, 2003, **46**, 967–977.
33 K. Kawai, Y. Osakada, M. Fujitsuka and T. Majima, *J. Phys. Chem. B*, 2008, **112**, 2144–2149.
34 H. W. Zimmermann, *Angew. Chem., Int. Ed. Engl.*, 1986, **25**, 115–130.
35 R. W. Armstrongy, T. Kurucsev and U. P. Strauss, *J. Am. Chem. Soc.*, 1970, **92**, 3174–3180.
36 M. K. Sarangi and S. Basu, *Phys. Chem. Chem. Phys.*, 2011, **13**, 16821–16830.
37 V. Kumar, A. Pandey and S. Pandey, *ChemPhysChem*, 2013, **14**, 3944–3952.
38 R. Wang, L. Yuan, H. Ihmels and D. H. Macartney, *Chem. – Eur. J.*, 2007, **13**, 6468–6473.
39 M. S. Ibrahim, I. S. Shehatta and A. A. Al-Nayeli, *J. Pharm. Biomed. Anal.*, 2002, **28**, 217–225.
40 G. Zhang, Y. Pang, S. Shuang, C. Dong, M. M. F. Choi and D. Liu, *J. Photochem. Photobiol., A*, 2005, **169**, 153–158.
41 G. Zhang, X. Hu, N. Zhao, W. Li and L. He, *Pestic. Biochem. Physiol.*, 2010, **98**, 206–212.
42 C. Y. Huang, *Methods Enzymol.*, 1982, **87**, 509–525.
43 M. Sayed, F. Biedermann, V. D. Uzunova, K. I. Assaf, A. C. Bhasikuttan, H. Pal, W. M. Nau and J. Mohanty, *Chem. – Eur. J.*, 2015, **21**, 691–696.
44 J. M. Schuette, T. T. Ndou, A. M. de la Pela, S. Mukundan Jr. and I. M. Warner, *J. Am. Chem. Soc.*, 1993, **115**, 292–298.
45 J. Carlstedt, A. González-Pérez, M. Alatorre-Meda, R. S. Dias and B. Lindman, *Int. J. Biol. Macromol.*, 2010, **46**, 153–158.
46 Y. Huang, Q. Lu, J. Zhang, Z. Zhang, Y. Zhang, S. Chen, K. Li, X. Tan, H. Lin and X. Yua, *Bioorg. Med. Chem.*, 2008, **16**, 1103–1110.

Open Access Article. Published on 26 February 2015. Downloaded on 2/25/2026 10:40:43 AM.
This article is licensed under a Creative Commons Attribution 3.0 Unported Licence.

47 M. Ageno, E. Dore and C. Frontali, *Biophys. J.*, 1969, **9**, 1281–1311.
48 T. O'Connor, S. Mansy, M. Bina, D. R. McMillin, M. A. Bruck and R. S. Tobias, *Biophys. Chem.*, 1981, **15**, 53–64.
49 C. M. Muntean, G. J. Puppels, J. Greve, G. M. J. Segers-Nolten and S. Cinta-Pinzaru, *J. Raman Spectrosc.*, 2002, **33**, 784–788.
50 F. Zsila, Z. Bikádi and M. Simonyi, *Org. Biomol. Chem.*, 2004, **2**, 2902–2910.
51 F. Mendicuti and M. J. González-Álvarez, *J. Chem. Educ.*, 2010, **87**, 965–968.
52 M. Shaikh, J. Mohanty, M. Sundararajan, A. C. Bhasikuttan and H. Pal, *J. Phys. Chem. B*, 2012, **116**, 12450–12459.
53 Q. Wang, R. He, X. Cheng and C. Lu, *J. Inclusion Phenom. Macrocyclic Chem.*, 2011, **69**, 231–243.
54 K. Fukui, K. Tanaka, M. Fujitsuka, A. Watanabe and O. Ito, *J. Photochem. Photobiol., B*, 1999, **50**, 18–27.
55 K. Fukui and K. Tanaka, *Angew. Chem., Int. Ed.*, 1998, **37**, 158–161.
56 J. Joseph, N. V. Eldho and D. Ramaiah, *Chem. – Eur. J.*, 2003, **9**, 5926–5935.
57 J. R. Lakowicz, *Principle of fluorescence spectroscopy*, Plenum Press, Springer, New York, 2006.
58 H. Joshi, A. Sengupta, K. Gavvala and P. Hazra, *RSC Adv.*, 2014, **4**, 1015–1024.
59 N. Nikolis, C. Methenitis and G. Pneumatikakis, *J. Inorg. Biochem.*, 2003, **95**, 177–193.
60 P. K. Singh and S. Nath, *J. Phys. Chem. B*, 2013, **117**, 10370–10375.
61 D. V. O'Connor and D. Phillips, *Time Correlated Single Photon Counting*, Academic Press, New York, 1984.